Detection of Fine-Scale Coherent Structures in a High-Reynolds-Number Turbulent Flow

Koji Sassa
Kochi University, Kochi, Kochi 780-8520, JAPAN

Fine-scale coherent vortices are tried to experimentally detect in a fully-developed turbulent flow at a high turbulence Reynolds number, $R_\lambda = 280$. Instantaneous velocity fields are measured using a multisensor with 21 I-probes. Instantaneous distributions of velocity gradients represent the existence of coherent vortices passing through the sensor. Characteristics of the fine-scale vortices shown by DNS were confirmed in the present experiment.

Key Words: Turbulent Flow, Flow Measurement, Fine-scale Vortex, Multisensor

1. Introduction

Recent DNS works found fine-scale coherent vortices existing only in turbulent shear flows[1] but also in. isotropic turbulence[2)~5)]. These fine-scale coherent vortices are regarded as the principal element of turbulence and play an important role in energy dissipation. The DNS turbulence fields had, however, relatively low Reynolds numbers, R_λ<100, and their energy spectra did not have wide inertial subrange. As for experimental works, they have just started. Maurer et al.[6] observed coherent vortex filaments by the concentration of air bubbles. Some quantitative results were obtained by using laser techniques, i.e. Relief[7] and DPIV[8]. Though one[7] of these experiments was performed even at the high Reynolds number, R_λ~360-600, they just showed the instantaneous transverse velocity profiles of coherent vortices and more detailed data are to be required.

The present work aims to detect these fine-scale coherent vortices in a high-Reynolds-number turbulent flow by using a multisensor probe and conventional hotwire bridges. The hotwire anemometry is an old-fashioned method but is the most reliable method. The continuous velocity data obtained from the multisensor are available to analyze statistical turbulence property related to the coherent vortices as well as to detect them. In this paper, I will show the possibility of multisensor for detecting coherent vortices as the first step of my work.

2. Experiment

The present experiment was carried out in a blow down type wind tunnel with an active turbulence grid. The test section is 35×45 cm^2 in cross section and 3.1 m long. The active turbulence grid[9] is a kind of biplane grid composed of 32 agitator rods with many triangular wings. Its mesh size, M, is 25 mm. Randomly oscillated the agitator rods with stepping motors, the air flow passing through it is effectively stirred and intense large-scale turbulence is induced in the test section. Its mean velocity, U, was 5 m/sec. The basic statistical properties of the resultant fully-developed turbulent flow were checked by using an X-wire probe and constant temperature hotwire anemometers.

The multisensor probe shown in Fig.1 was newly designed to get instantaneous cross sectional velocity distributions. It has 21 I-wire sensors made of Tungsten wire of 2.5 μm in diameter and 05 mm long. The interval of each sensor is 1 mm and 5 times as large as Kolmogorov dissipation scale, η. The frontal area of the probe is 4.5× 4.5 mm^2 and just slightly larger than that of the conventional commercial I-probe. As for measuring mean velocity and turbulence intensity, there is little difference between the X-wire probe and the multisensor probe. In the present experiment, central 9 sensors were connected with constant temperature hotwire bridges and surrounding 12 sensors were dummies. The probe was settled at the center of the cross section at X/M=80 where the turbulence field was fully developed as mentioned later. The outputs of the

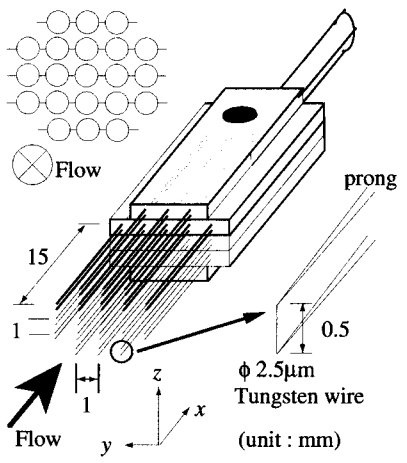

Figure 1. Multisensor Probe

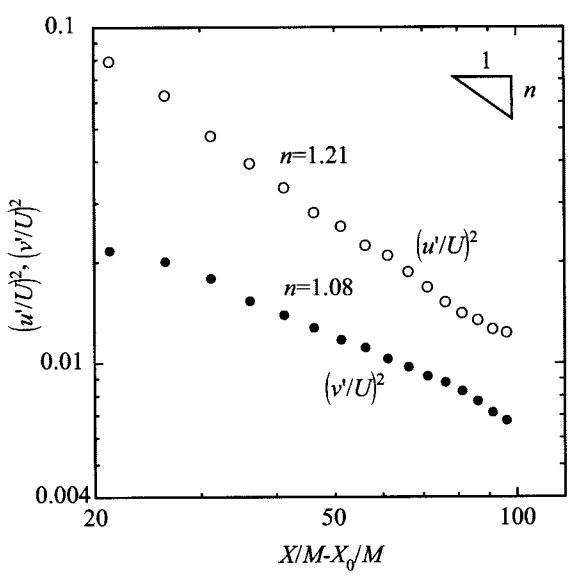

Figure 2. Streamwise decay of turbulence energy

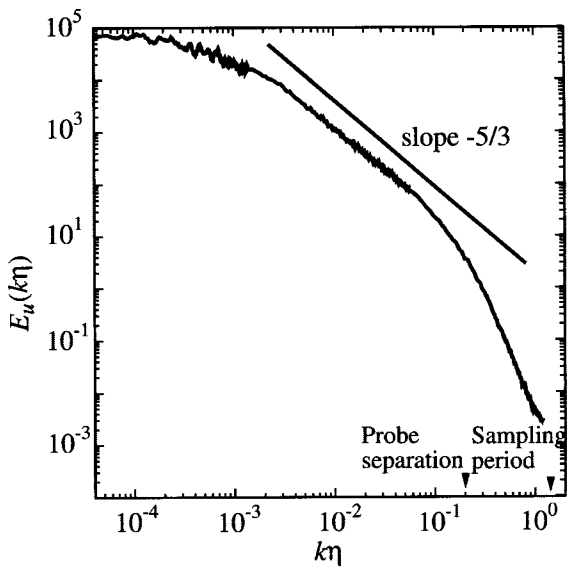

Figure 3. One-dimensional energy spectrum at X/M=80

bridges were sampled for 5 minutes by a 16bit A/D converter at 20 kHz in sampling frequency and then linearized by a personal computer. The velocity gradients, du/dx(=du/Udt), du/dy and du/dz, were calculated from the 9 time series of the digitized longitudinal velocity. Wavelet analysis was also performed with respect to these data.

3. Statistical property of turbulence field

Figure 2 shows streamwise decay of longitudinal and lateral components of turbulence energy. Energy decay clearly obeys the power law for X/M>50. The exponent, n, denoting the decay rate of turbulence energy was 1.20 and 1.09 for the longitudinal and lateral components, respectively. These values are almost the same as the results of the conventional grid turbulence[10]. The turbulence intensity was, however, one order of magnitude larger than that of the grid turbulence, for example, u'/U=13.6% at X/M=80 as shown in Table 1. The present active turbulence grid excited the longitudinal component more effectively than the lateral component, so that the anisotropy, u'/v', was about 2.0 at X/M=20. The present turbulence field returned to isotropy downstream. Though the anisotropy still remained by the end of the test section, it appeared only in low wave number range and local isotropy was well satisfied for the inertial and viscous subranges[11]. The relatively downstream point (X/M=80) where the turbulence confirmed the decay law and had still large turbulence Reynolds number, R_λ=289, was decided as the measuring point.

Table 1. Characteristics of turbulence at X/M=80

U(m/sec.)	u'/U	η (mm)	λ (mm)	R_λ
5	0.136	0.2	7.3	289

One-dimensional energy spectrum of longitudinal velocity fluctuation at X/M=80 is shown in Fig. 3. Inertial subrange is clearly observed for more than one decade wave number range. The probe separation and sampling period are also shown in this figure. The sampling period of A/D converter has sufficiently high resolution to investingate this turbulence field, but the probe separation is just the smallest possible size at the present time.

4. Results and Discussion

The instantaneous longitudinal velocity data obtained from 9 sensors were almost same with each other except for small scale and high frequency fluctuation, as

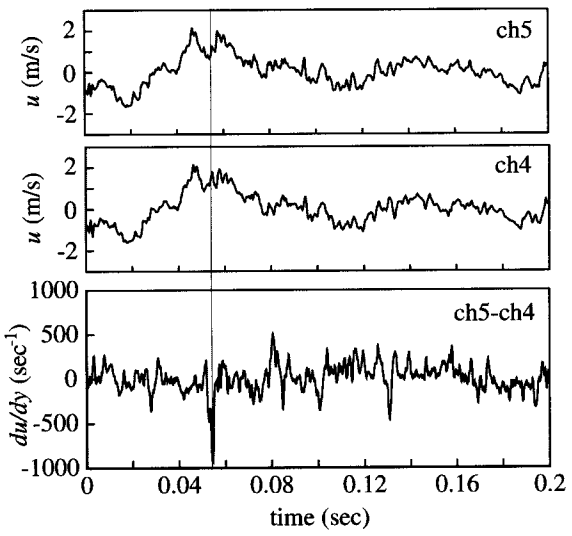

Figure 4. Wave Traces of Velocity Fluctuations of Ch.4 and Ch.5 and Velocity Gradient, du/dy

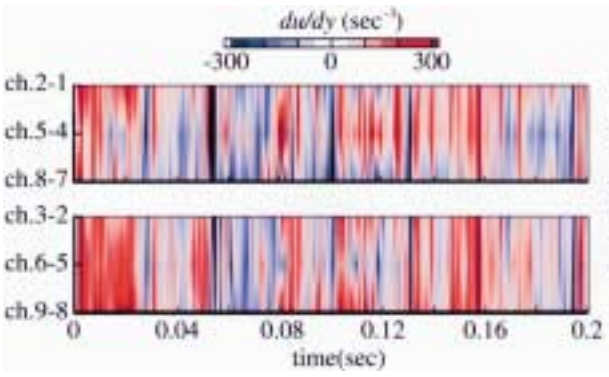

Figure 5. Contour maps of *du/dy*

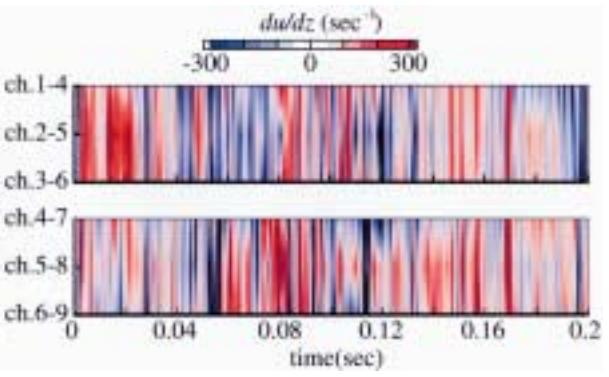

Figure 6. Contour maps of *du/dz*

shown for Ch.4 and Ch.5 in Fig.4. The velocity difference at high frequency between Ch.4 and Ch.5 is shown as the local velocity gradient, *du/dy*, in the bottom figure of Fig. 4. High shear events such as pointed by line at 0.054 sec. are observed to occur intermittently. Unfortunately, the probe can measure the instantaneous distribution of longitudinal velocity component only and I could not employ the vortex identification schemes, e.g., high enstrophy region[3], low pressure region[4], second invariant of velocity gradient tensor[1]. For the sake of convenience, the high shear events were regarded as the high vorticity region passing through the probe.

Figures 5 and 6 show the contour maps of *du/dy* on *x-z* planes and the contour maps of *du/dz* on *x-y* planes, respectively. Though there are high shear spots, many high shear regions apparently extend spanwise. Such spanwise extent of high shear region is thought to represent the intermittent passage of fine-scale coherent vortices through the probe. Comparing Figs. 5 and 6, the intensity of velocity gradient is found to be almost same between them. This fact shows that the spanwise resolution of the present multisensor probe is independent of the direction of I-wire.

If the high *du/dx* region is regarded as the high strain rate region in the same manner for the vorticity, it also represents the high dissipation region. As shown in the top and bottom maps of Fig. 7, energy dissipation is found to intermittently occur in high wave number range of $k\eta > 0.05$. The high vorticity is observed close to the high dissipation regions though it exists even in the lower inertial subrange of $k\eta \sim 0.005$. The high vorticity regions where the amplitude is larger than 1.5 times of rms. vorticity occupied only 10% of total sampling time, but the energy dissipation conditioned by the high vorticity region was twice of mean energy dissipation. These fact supports the DNS results which fine-scale vortices contribute to the energy dissipation[5]. Figure 8 shows the scale dependence of *du/dy* and *du/dx*. In the viscous subrange of $k\eta = 0.16$, thin high vorticity regions extending across the probe width are found to be accompanied by the high enegry dissipation. With the present detection scheme, the fine-scale coherent vortices are observed even in the inertial subrange of $k\eta = 0.039$ and 0.0098, but they do not contribute to energy dissipation at all. Of course, these maps denote just relative wavelet amplitude and the intensity of the coherent vortices become weaker in the lower wavenumber range.

The high vorticity regions and high dissipation regions are mapped in Fig. 9. The threshold is 1.5 times of r.m.s. values. Though there are isolated high vorticity or high dissipation regions, most of the regions in which the vorticity is concentrated align normal to the mean flow direction. These regions like cylinders with high vorticity are regarded as fine-scale coherent vortices passing through the probe as illustrated in the figure. This figure may include subjectivity more or less, but at least the existence of fine-scale coherent vortices was confirmed in the actual high Reynolds number turbulent flow. The mean diameter of the coherent vortices was about 10η, which supports DNS results[1)4)]. As for the length of the fine-scale coherent vortices, the DNS argued the order same with the integral scale[1]. The multisensor probe covers only one-half

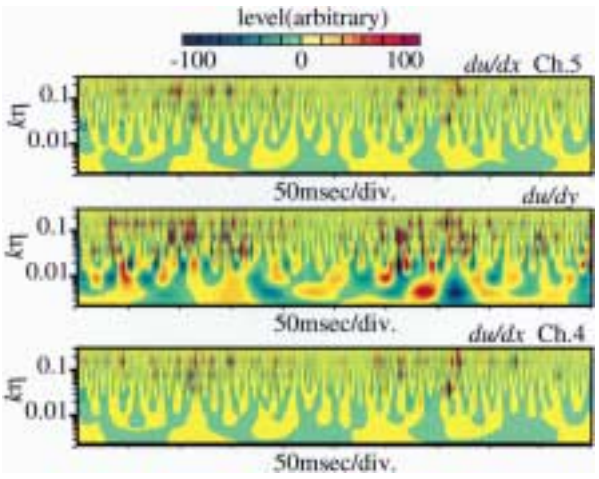

Figure 7. Wavelet transform of velocity derivative, *du/dx*, at Ch.4 and Ch.5, and velocity gradient, *du/dy*.

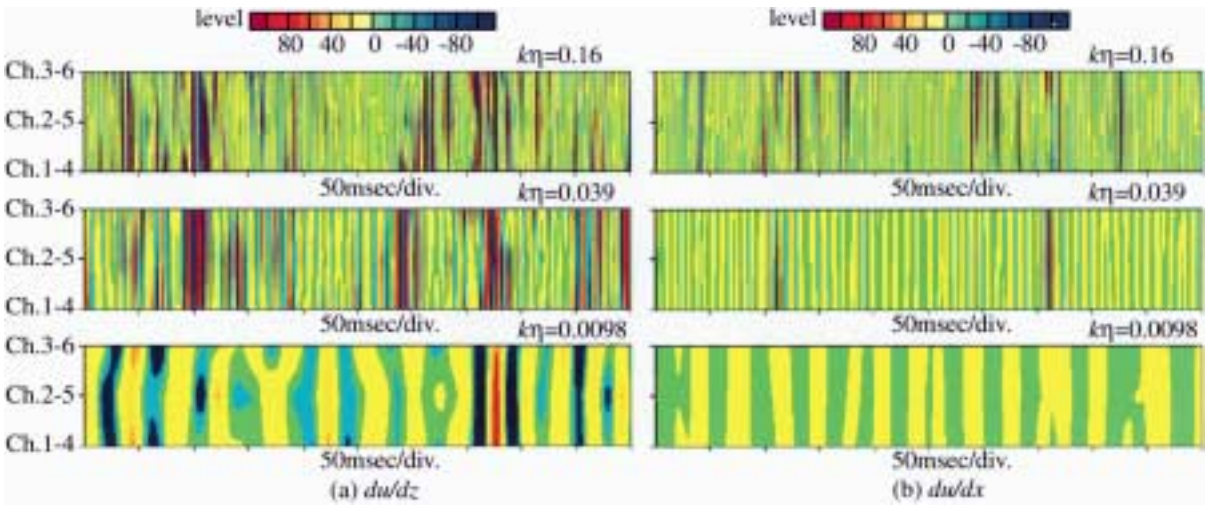

Figure 8. Contour maps of wavelet amplitude of *du/dz* (a) and *du/dx* (b).

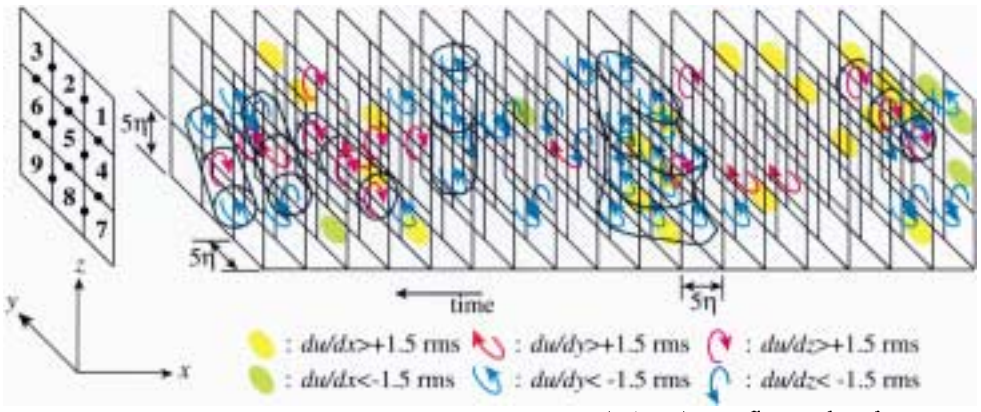

Figure 9. Three-dimensional plots of high velocity gradients. Cylinders denote fine-scale coherent vortices.

of Taylor's microscale, then the verification of the vortex length is one of future subjects.

5. Concluding remarks

Fine-scale coherent vortices were experimentally detected by using a multisensor probe in a fully-developed turbulent flow. Their characteristics, such as the diameter and the contribution to the energy dissipation, are similar to those obtained by DNS studies.

In order to identify the coherent vortices more objectively, it is necessary to improve the multisensor; i.e., making their resolution higher and enabling to measure the other velocity components.

Acknowledgments

I am grateful to Prof. Nishioka and Prof. Tatsumi for helpful suggestions. This work has been supported in part by the Grant-in-Aid (C) (2) No.10650180 from the Japanese Ministry of Education, Science, and Culture.

References

1) Tanahashi,M., Miyauchi,T. and Ikeda,J., *Proc. of IUTAM Symp. on Simulation and Identification Organized Structures in Flows*, pp.131 (1999).
2) Yamamoto,K. and Hosokawa,I., *J. Phys. Soc. Japan*, 57 pp.1532 (1988).
3) Vincent,A. and Maneguzzi,M., *J. Fluid Mech.*, 225 pp.1 (1991).
4) Kida,S. and Miura,H., *J. Phys. Soc. Japan*, 67 pp. 2166 (1998).
5) Brachet,M.E., *Fluid Dyn. Res.*, 8 pp.1 (1991).
6) Maurer,J., Tabeling,P. and Zocchi,G., *Europhys. Lett.*, 67 pp.983 (1994).
7) Noullez,A., Wallace,G., Lempert,W., Miles,R.B. and Frisch,U., *J. Fluid Mech.*, 339 pp.287 (1997).
8) Tanahashi,M., Fukushima,M. and Miyauchi,T., *RIMS Kokyuroku* , 1141 pp.184 (2000) (in Japanese).
9) Makita,H. and Sassa,K., *Adavances in Turbulence* 3 pp.495 (1991).
10) Comte-Bellot,G. and Corrsin,S., *J. Fluid Mech.*, 25 pp.657 (1966).
11) Sassa, K., Matsunaga,S. abd Makita,H., *Adavances in Turbulence* VIII pp.291 (2000).